PROCEEDINGS OF SPIE REPRINT

SPIE—The International Society for Optical Engineering

Reprinted from

Optical Fiber and Fiber Component Mechanical Reliability and Testing

6–7 November 2001
Boston, USA

Volume 4215

P.O. Box 10, Bellingham, Washington 98227 USA. Telephone 360/676-3290.

New Silica Optical Fibers with Nano Porous Silica Cladding/Coating

Bolesh J. Skutnik

Fiber Optic Fabrications, Inc. and CeramOptec Industries, Inc., East Longmeadow, MA 01028

ABSTRACT

A new type of optical fiber has been developed with all pure silica in both core and cladding. The cladding is a nano porous silica produced on line from an oligimeric organo-silicate by a modified sol-gel technology. Characteristics, mainly mechanical properties, are described. The strength and fatigue of these optical fibers are very good, even without additional protective jackets. The nano porous silica is also being evaluated as an outer coating on all silica optical fibers. Unjacketed fibers have mean Weibull strengths in bending of 6.5 to 7.6 GPa with Weibull slopes in the 40 to 60 range. Strength decrease with decreasing strain rate is similar for both jacketed and unjacketed fibers. Static fatigue results using mandrel wrap tests are also presented. Dynamic and static fatigue parameters appear to be essentially the same with values around 20. A thin polyimide jacket does improve some of the mechanical properties. Results for nano porous silica 'buffer' over a silica/fluorosilica core clad structure are also presented. Effects of water and dry environments are presented, including results of short to intermediate term aging in boiling water. Possible mechanisms to explain the strength and fatigue behavior are discussed in light of these fibers' unique structure.

Keywords: sol-gel clad optical fibers, nano porous silica clad optical fibers, high strength high temperature fibers

1. INTRODUCTION

In 1993 a new approach to "sol-gel" material processing was discovered[1]. As an outgrowth of this discovery, it was found that micro porous silica could be produced on a pure silica core, such that a truly functional optical fiber was fabricated[2]. These experiments were an outgrowth of work begun in the 1980s[3-5]. Overall objectives of this research has been to develop radiation resistant multi mode optical fibers for extra-terrestrial applications, such as space satellites, and to establish the advantages of a nano porous clad pure silica core optical fiber as a specialty optical fiber for new applications such as a substrate for active photonic devices and for delivery and activation of active chemicals for Photo-Dynamic Therapy.

Unlike normal all-silica optical fibers which require a buffer or jacket to protect the silica outer surface from environmental exposure to moisture and flaw initiating contacts, the nano porous clad fibers behave more like hard plastic clad silica (HPCS) optical fibers[6] in that they do not require a buffer or jacket over the cladding as a minimum structure for a viable, commercially useful optical fiber. As with HPCS fibers a jacket is beneficial for most practical environments[7,8].

In this paper primarily the mechanical properties of the nano porous silica clad optical fibers, including the strength and fatigue properties of these fibers are presented. Some optical properties will be mentioned to complete the information on thee new optical fibers. The effects of boiling water on the strength behavior of these optical fibers are presented and discussed. Preliminary experiments devised to introduce into the nano porous silica photoactive chemicals and then activating them will be discussed. Potential new applications as a substrate for various telecommunication and biotechnology areas are suggested.

2. EXPERIMENTAL

The material used as a precursor is a hydroxy, ethoxy terminated ladder oligimer with significant Si-C

Optical Fiber and Fiber Component Mechanical Reliability and Testing, M. John Matthewson, Editor, Proceedings of SPIE Vol. 4215 (2001) © 2001 SPIE · 0277-786X/01/$15.00

linkages as methyl groups attached to silicon[9]. It was applied from a 50/50 solute/solvent by weight ethyl acetate solution for data reported here. A polymeric jacket, when applied, consisted of a single coat of a polyimide applied 'in line' but after the nano porous clad optical fiber came off the draw tower.

The nano porous silica clad optical fibers were drawn on conventional fiber draw towers[10] using thermal ovens to cure/convert the precursor materials to the nano porous silica cladding/coating. Typically temperatures in the range of 450 to 700 ^{0}C were employed. Conversion of the silica precursor to nano porous silica is done in line. Draw speeds of 7 to 70 meters/min have been employed to date. Typical residence time in a given oven is 0.5 to 5 seconds with a total time of exposure to elevated temperatures of approximately 5 to 30 seconds. As used in this paper in line processing refers to processing before the optical fiber is diverted from vertical travel, i.e. before the fiber comes in contact with the pinch wheel at the bottom of the draw tower. When used, 'in line' processing refers to processing occurring during the original fiber draw process but after the fiber has been diverted from vertical travel.

For results described below, a double application was used with a final sol-gel coating/coating thickness of 12 to 15 μm. The size of the solid silica core varied among the runs from diameters of about 100 μm to about 200 μm. Most recently some fibers were made where the nano porous silica was applied over a silica/fluorosilica core/clad fiber, having dimensions of 278/304 for the synthetic silica layers. The actual dimensions of specific data are given with the figures displaying results. The core silica material in all cases is a low-OH undoped silica, typically less than 5 ppm of OH. When applied, the jacket material was a single coat of a polyimide, cured by a series of ovens ranging in temperature from 300 to 500 ^{0}C. Polyimide thickness was generally ~7 μm.

The two point bend tests were performed on a 2-point bend tester with grooved stainless steel faceplates holding up to 10 fibers at a time. Measurements of strength and dynamic fatigue were made at constant strain rates of 10%/min down to 0.05%/min and under ambient conditions, which were typically 23 ^{0}C and 35 to 60 % RH. Samples tested in ambient water were immersed in water and the testing began within a minute with the exception that the polyimide jacketed fiber was held in the water for 15 minutes before running the 10%/min tests.

Two point bend strength testing has been described in the literature[11-13]. Note that the gage length for this type of test is small, on the order of a few millimeters. The data in Figure 1 represents breaks from over 220 samples. These come from several fiber draws representing >20 km from which the smaller sections of samples have been taken for actual testing. The data in the other figures represent a sample of 30 per case and thus represent less than 0.25 meter of fiber actually tested. These samples, however, were normally not taken all in a row. Rather, large sections of fiber were drawn between sets of ten (10) samples.

The fibers exposed to boiling water were immersed in an open container filled with deionized water, which was held at a rolling boil for 1 or 8 hours. After the exposure to boiling water, the fibers were removed and allowed to stand at ambient condition overnight before testing. For testing, fibers were loaded into the grooved faceplates, using 10 fibers per stress test. Loading times from the first fiber to the tenth took about 4 minutes; ambient testing environment was 23 ^{0}C and 35 to 60% RH.

Static fatigue measurements were performed by the mandrel wrap method[14-16]. The length of fiber under test was about 500 mm. The fibers were wound in ambient conditions [23 ^{0}C; 35 to 60% RH] and tested in ambient water [T = 23 ^{0}C]. Mandrel diameters were selected to yield stresses between 1.4 and 4.6 GPa [200 to 667 kpsi]. A minimum of five samples were used for each mandrel size and at least four different mandrel sizes were used for each fiber run tested.

3. RESULTS

3.1 Two-Point Bend Strength Tests

Figure 1 presents data from several fiber draws where over 220 samples were tested out of >20 km of fiber produced under equivalent conditions over a twelve month period. Except for the very strongest values the curve is rather steep. There appears to be no real breaks in the slope, indicating a single flaw distribution.

Figures 2, and 3 present the change in Weibull strength as the constant strain rate is changed for tests run in ambient air, and in ambient water, respectively. In each figure the unjacketed fiber results are denoted by Xs, while the polyimide jacketed fiber results are denoted by open circles, Os. As can be seen the jacketed fiber

results are generally steeper in slope than the unjacketed fiber results. Curves for the jacketed and unjacketed fibers are very close to one another in ambient water testing (Figure 3).

Figure 4 presents a summary of the affect of exposure to boiling water prior to testing in ambient air conditions. Fiber samples were allowed to re-equilibrate with ambient air conditions before being tested. The Weibull plot for the polyimide jacketed fiber did not change substantially after either aging exposure. The unjacketed sol-gel clad fiber remained unchanged after the one hour exposure, however, it changed rather dramatically after the eight hour exposure to boiling water. The low strength end of the unjacketed fibers strength curve shows a definite broadening of the flaw population.

Figure 5 presents data for a nano porous silica coated fiber with a larger cylinder diameter for the coating. The fiber is a pure, high OH silica core, a fluorosilica cladding with the nano porous silica as a coating over the fluorosilica cladding and with a polyimide jacket. The ambient air, 45% RH, sample fibers and those tested in ambient water have very similar Weibull plots, with just a reduction in mean strength of about 0.3 GPa. Testing in boiling water notably reduces the mean strength to about 4.5 GPa or about 2 GPa below the ambient air tests. The appearance of a weak strength tail is also seen to be beginning.

3.2 Static Fatigue Tests

The results for ambient water immersion include moderately long term failures with all the initial samples of the unjacketed fiber having been broken. In Figure 6 the time to failure for samples of an unjacketed fiber are presented. The data points clearly show a break in the curve with the lower stresses breaking earlier than predicted by the short term results. The trend in the short term data in Figure 6 indicates a static fatigue parameter, N_S, of about 18 for the unjacketed sol-gel clad optical fiber. This is a common magnitude for a variety of acrylate jacketed optical fibers[8,11] over a similar time to break range. Above the break at longer times, the static fatigue parameter has dropped to a value of about 3. Further comments appear below in the Discussion section.

In Figure 7 the upper squares represent the time to failure for the polyimide jacketed sol-gel clad optical fiber. Triangular points at the top of the figure represent samples which had not broken when this graph was prepared about 570 days, >13,500 hours, into the testing program. Note that at given stresses the failure times are longer for this fiber than for the unbuffered fiber. The scatter of the data is somewhat diminished and the static fatigue parameter is 21. Also note that the highest stress tested is over 4.6 GPa [660 kpsi].

3.3 Modification/Use of Nano Porous Clad Structure

Two studies are underway at University related laboratories to explore the doping or modification of the nano porous structure of the coating/coating to provide either active sites for chemical or biological activity or for sensing applications. Thus far, results have been received indicating the attachment of Rhodamine complexes which could be activated by light energy transmitted down the fiber to the sites where the complexes were 'incorporated'. Also in the second study gratings have been formed within the nano porous structure through the use of photo activated precursors. The quality of grating permitted the entry and exit of signals through the grating sections which were deposited and created within the sol-gel derived nano porous cladding. Preliminary studies indicated that the nano porous structure has very small voids internally while the surface appears to be contiguous. Although high resolution microscopy has confirmed that the photo-activated grating material was within the nano porous silica cladding not merely on the surface of the cladding. Semi-quantitative results on some of the early phase II fibers indicated that the median pore size was on the order of 30-40 nm. This has lead us to refer to these fibers as nano porous rather than micro porous as was done earlier in the development.

4. DISCUSSION

4.1 Two-Point Bend Strengths vs. Strain Rates

The results in Figure 1 demonstrate the consistency of the results obtained from a large number of fiber draw runs, i.e. a large number of silica rods and sol-gel precursor preparations. Also as noted earlier since the gage length is short for two-point bend tests, it is useful to have an extensive number of tests over a large sampling of optical fiber to help validate the results observed in more limited sampling for the varying strain rate

data Figures 2 and 3. The samples tested for Figure 1 represent a random sampling of over 20 kilometers of modified sol-gel clad optical fiber. A main feature of Figure 1 is the steepness of the slope, especially in the upper region, which tends to imply that the flaw distribution may actually be unimodal[17].

The results of Figures 2 and 3 demonstrate the relatively equivalent behavior of the unjacketed sol-gel clad fibers and the polyimide jacketed fibers. At the two slowest strain rates the data for the unjacketed fiber clearly shows a discontinuity in the slope. The interesting point is that the plot of data below the 'kink' is as steep or steeper than the highest strength section of the plots. This could be interpreted as arising from possibly two nearly unimodal flaw distributions separated in size by a small amount.

The dynamic fatigue of unjacketed and polyimide jacketed fibers were determined from the results given above for the two conditions presented. Within experimental error the apparent dynamic fatigue parameter is $N_D = 22 \pm 2$ regardless of whether the sol-gel clad optical fiber is jacketed with polyimide or not.

4.2 Bend Strength Testing After Aging in Boiling Water

The results in Figure 4 indicate that exposure of the polyimide jacketed optical fibers to boiling water even up to eight (8) hours did not change the bend strength behavior of the fibers as long as time was allowed for the samples to return to room temperature and humidity before testing under these latter conditions. As noted the unjacketed fibers did not affect the strength after a one-hour exposure, however significant changes occurred after the 8 hour exposure. Here the low strength end of the unjacketed fibers strength curve shows a definite broadening of the flaw population, showing some permanent changes in the flaw distribution for the 8-hour boiled fiber samples. The defect size distribution appears to have broadened significantly with the extended time in the boiling water. This behavior, though, is still quite remarkable for an unjacketed optical fiber, namely, being able to withstand over an hour exposure to boiling water before samples experienced even a 10% loss if strength, when tested at ambient after allowing an overnight recovery period.

4.3 Bend Strength Testing in Ambient and Boiling Water

The results in Figure 5 confirm the observations found in Figures 2 and 3, namely that the polyimide jacketed optical fibers have very similar strengths whether tested in ambient air or in ambient water. Further the strength measured in boiling, while significantly lower, is not catastrophically reduced. The mean strength drops from about 6.5 GPa (935 kpsi) down to about 4.5 GPa (650 kpsi). As might be expected the weak strength end is beginning to show a tail to lower strengths. In tests with the smaller core/clad fibers not presented here, more extensive testing indicates a sharpening of curve in the lowest strengths much as seen at slower strain rates in Figure 3. Also in other testing, in agreement with the data found in Figures 2 and 3, unjacketed nano porous clad/coated fibers were found to be substantially the same as shown here for the jacketed fibers.

4.4 Static Fatigue Behavior

By their nature static fatigue measurements usually yield much longer times to failure and thus sample experience much longer exposure to the test environment than in dynamic fatigue testing. Small differences in the fatigue behavior of similar samples become more pronounced in static fatigue testing. Furthermore in studies, like the present one, where dynamic measurements are made by the two point method, the gage length of the static fatigue samples are generally longer than for the dynamic fatigue samples. The two features greatly enhance the observation of differences in sample behavior by static fatigue testing over dynamic fatigue testing. The appearance of a 'knee' in the data plotted in Figure 6 for the unjacketed fiber samples is an example of this phenomenon. This 'knee' is a well recognized feature of the standard telecom optical fibers and many other fibers as well. The research groups at Bell Labs and at Rutgers University[11,18,19,20] and others[21] have reported on the occurrence and significance of this feature. The 'knee' feature was found present in bare fiber work and in most acrylate jacketed optical fibers.

It should be noted that neither the ambient water data nor the boiling water data for the polyimide jacketed fibers show a clear break (or knee) in the their plots. The absence of a break in the static fatigue test results has been reported earlier for Hard Plastic Silica Clad optical fibers[6] and some silicone clad/coated fibers[13]. To be sure that this is the case for these polyimide jacketed fibers, we still need to document failure times for the unbroken fibers on medium stress mandrels. These are the samples where one or two samples have broken but

several additional samples have remained unbroken for over a year and a half. Final judgment on the long term behavior for these jacketed fibers awaits completion of the tests.

4.5 Nano Porous Structure

The basic science and engineering studies are underway which utilize the nano porous structure to incorporate other materials which in turn permit the modified sections to interact with the surrounding environment and transmit a modified signal. Preliminary tests have established that complexes such as Rhodamine can be activated by signals traveling in the fiber core after incorporation of the complex in a section of the modified sol-gel clad fiber. The guided waves within the fiber core extend a distance into the cladding. Where the complex is incorporated into the cladding, it can interact with the waves travelling within the core and become activated.

The new studies underway look to explore further these effects to design and construct sensors for various chemical and biochemical moieties. We are looking at several different processing conditions and other variables to create nano pores of different sizes for use with materials of differing dimensions.

4.6 Considerations for Active and Passive Applications

There are a number of ways the nano porous structure could be used in biotechnological applications. The simplest might be to modify a fiber tip for photodynamic therapy by adjusting the refractive index in the tip section to scatter light laterally from the tip section. A grating technology similar to that mentioned above could be incorporated to deflect light out in the area of the grating. It might even be possible to incorporate a species which could initiate the therapy by direct activation of the species within a cladding section.

Placement of luminescent or other sensing moieties into the nano porous cladding/coating would permit such sections to sense specific aspects of body tissue or fluid in contact with the modified section of optical fiber. In a somewhat analogous manner a highly toxic or active material might be introduced into a living body in a relatively inactive form. Upon reaching a desired site for treatment, the material could be remotely activated by a laser or other photonic signal.

In non medical areas, the gratings could be used to add or subtract signals from the main transmission without necessarily creating a break in the main line. Evanescent coupling would also be possible in such scenarios. Active fiber sections should be possible, achieved by doping the nano pores with light active, electro active or magneto active materials. The small size of the pores would create new constructions, which could enhance desired properties such as non-linear behavior, magneto-restrictive behavior or generation of local electromagnetic fields.

These few suggestions could lead to a large number of specific applications within the medical field, ranging from direct treatments to sensing dosage of radiation delivery procedures to locating specific tissues, such as cancerous tissue, through minimally invasive techniques.

Additional characterization work is still necessary along with studies of modifications to fiber sections to achieve specific results in body tissue and fluids. We hope to continue to report on the properties of this new type of optical fiber as the data are generated and verified. Sample optical fibers are available for studies by potential end users.

ACKNOWLEDGMENTS

The author gratefully acknowledges receiving support for this work from the US Army through its Communications and Electronics Command under contracts DAAB07-95-C-D009 and DAAB07-96-C-D612. The author thanks B.G. Bagley, S. DiVita and W. Neuberger for helpful discussions and comments on this work. The author is grateful to S. Johnson, M. Trumbull, A. Suchorzewski and H. Park for technical assistance.

REFERENCES

1. Work performed by CeramOptec, Inc. under a Cooperative Research and Development Agreement (CRADA) on D-shaped fibers with US Army's CECOM at Ft. Monmouth, NJ.

2. B.J. Skutnik and S. DiVita, "Pure Silica Optical Fibers Utilizing Sol-Gel Techniques", AFCEA Ann. Conference Proc. 369-73 (1996).
3. R.O. Savage, R.J. Fischer and S. DiVita, US Patent No. 5,114,738 (1992).
4. J.R. MacChesney, D.A. Pinnow and L.G. van Uitert, US Patent No. 3,806,224 (1974).
5. B.G. Bagley, P.K. Gallagher, W.E. Quinn and L.J. Amos, Mat. Res. Soc. Proc. **32**, 287 (1984).
6. B.J. Skutnik, SPIE **1893**, 2 (1993), and references therein.
7. J.P. Clarkin, B.J. Skutnik and B.D. Munsey, J. Non-Cryst. Solids **102**, 106 (1988).
8. T.S. Wei and B.J. Skutnik, J. Non-Cryst. Solids **102**, 100 (1988).
9. B.J. Skutnik and M.R. Trumbull, J. Non-Cryst. Solids **239**, 210 (1998).
10. Norsken 8 meter, 2 coating station, draw tower; Heathway 12 meter. 2/3 coating station, draw tower.
11. M.J. Matthewson, C.R. Kurkjian and S.T. Gulati, J. Am. Ceram. Soc. **69**, 815 (1986).
12. J.B. Murgatroyd, J. Soc. Glass Tech. **28**, 388 (1944).
13. D. Roberts, E. Cuellar, L. Middleman and J. Zucker, SPIE **721**, 28 (1986).
14. B.J. Skutnik, M.H. Hodge and D.K. Nath, in: FOC/LAN '85 Proc., 232 (1985).
15. B.J. Skutnik, M.H. Hodge and J.P. Clarkin, SPIE **842**, 162 (1987).
16. B.J. Skutnik and T.S. Wei, SPIE **842**, 41 (1987).
17. C.R. Kurkjian and U.C. Paek, Appl. Phys. Lett. **42**, 251 (1983).
18. C.R. Kurkjian, J.T. Krause and M.J. Matthewson, J. Lightwave Tech. **7**, 1360 (1989).
19. M.J. Mathewson, V.V. Rondinella and C.R. Kurkjian, SPIE Proc. **1791**, 52 (1992).
20. J.T. Krause, J. Non-Cryst. Solids **38&39**, 497 (1980).
21. E. Cuellar, M.T. Kennedy, D.R. Roberts and J.E. Ritter, Jr., SPIE Proc. **1791**, 7 (1992).

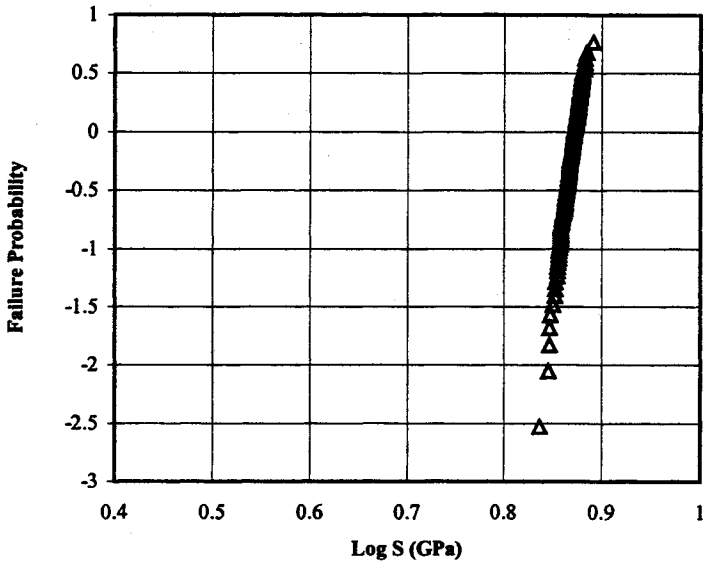

Figure 1: Weibull plot of the dynamic strength for unjacketed sol-gel clad optical fibers, having a pure silica core with diameter of 165 μm and a clad diameter of 195 μm; constant strain rate of 10%/min; 2-point bend test carried out in ambient air, ~23 ^{0}C 50% RH.

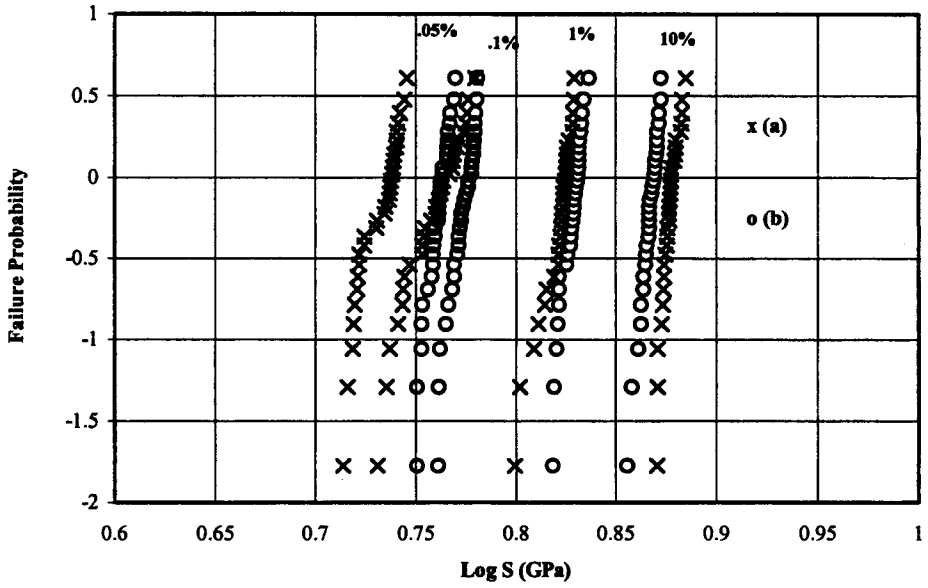

Figure 2: Weibull plots of dynamic strength measurements taken at strain rates varying from 10%/min down to 0.05%/min (a) unjacketed sol-gel clad optical fibers nominally 165/190 μm core/clad diameters, "x" points; (b) polyimide jacketed sol-gel clad optical fibers nominally 204/232/244μm core/clad/polyimide diameters, "o" points; 2-point bend test; ambient air = 23 ^{0}C, 35-60%RH

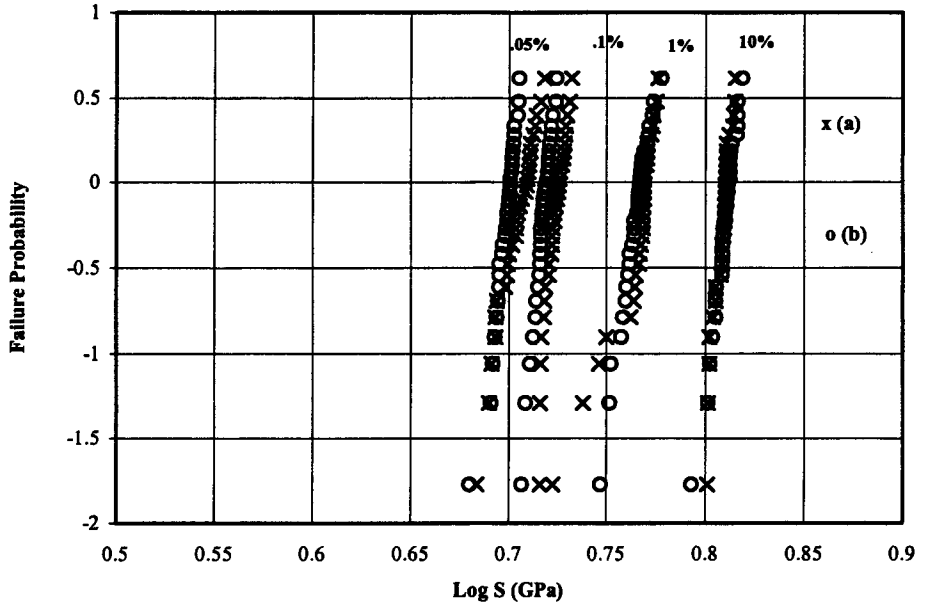

Figure 3: Weibull plots of dynamic strength measurements taken at given strain rates, "x" points for unjacketed fiber of Figure 2(a), "o" points for jacketed fiber of Figure 2(b); 2-point bend test; testing in ambient water, 23 ^{0}C.

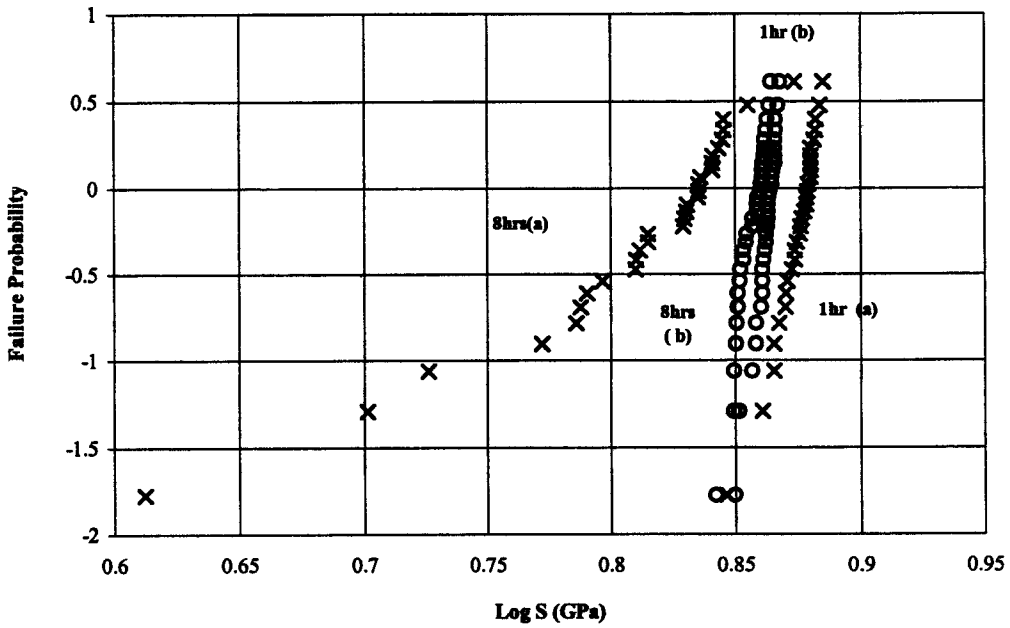

Figure 4: Weibull plots measured at the given strain rates, "x" points unjacketed fiber of Figure 2(a), "o" points jacketed fiber of Figure 2(b); 2-point bend test; testing in ambient air, 23 ^{0}C 35% RH, after immersion in boiling water for 1 hour or 8 hours and then drying overnight before testing.

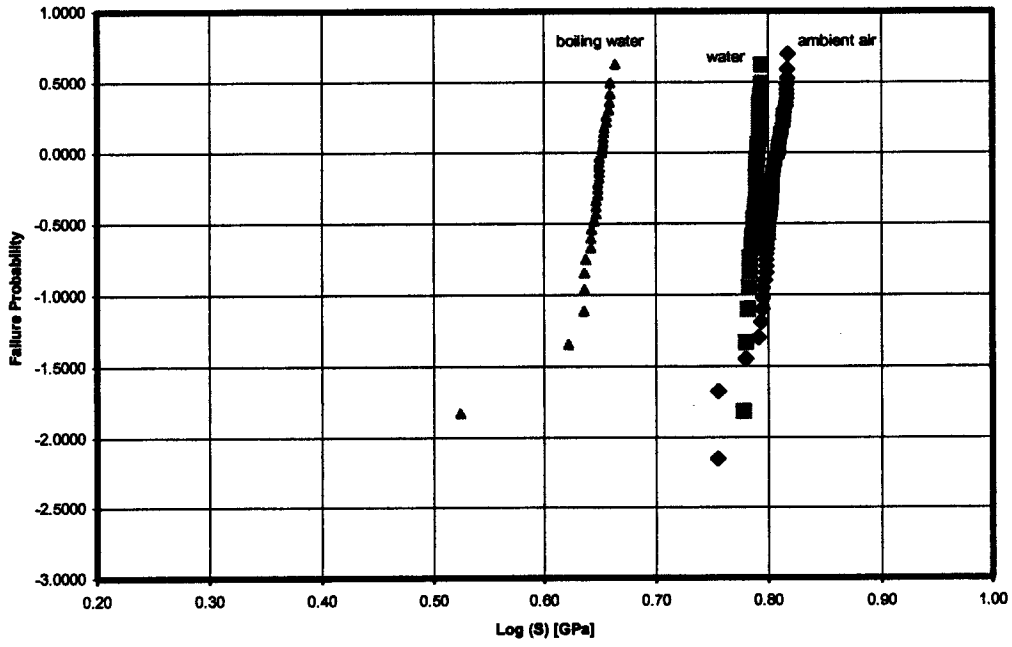

Figure 5: Weibull plot of the dynamic strength for polyimide jacketed sol-gel clad optical fiber, having silica core/clad with diameters of 278/304 μm, a nano porous silica coating with a 330 μm diameter and a polyimide jacket with a 355 μm diameter; constant strain rate of 10%/min; 2-point bend test carried out in ambient air, ~23 ^{0}C 45% RH [diamonds], in water [boxes], in boiling water [triangles].

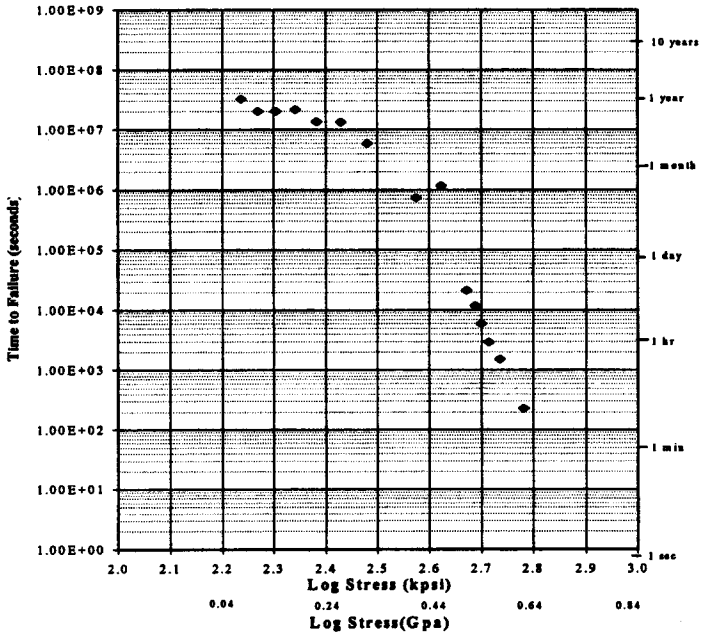

Figure 6: Static fatigue plots of failure times of 0.5 m length of sample fiber wrapped around mandrels giving the bending tensile stresses plotted, each point represents an average of the failure times of at least 5 samples for each stress level; "x" points for unjacketed fiber whose dimensions are 164/184 μm core/[sol-gel clad]; testing in ambient water, 23 ^{0}C; N_S (hi) = 18; N_S (knee) = 3.

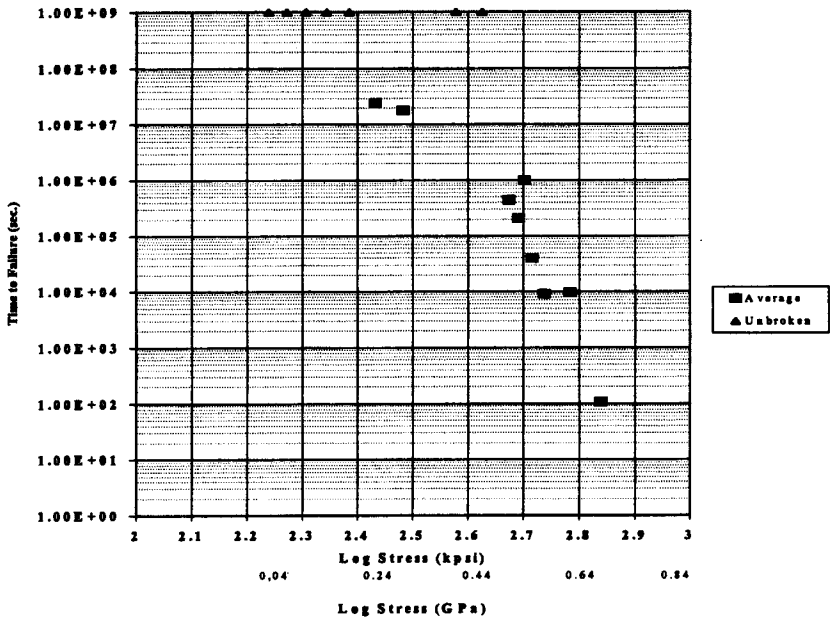

Figure 7: Static fatigue plots similar to Figure 6 for jacketed fiber whose dimensions are 162/192/208 μm core/[sol-gel clad]/polyimide; "boxes" points for fiber tested in ambient water, 23 ^{0}C; points at top of graph represent fiber samples which have not yet failed at the indicated stress levels; N_S (water) = 21.